Hepatobiliary & Pancreatic Diseases International 18 (2019) 38–47

Contents lists available at ScienceDirect

Hepatobiliary & Pancreatic Diseases International

journal homepage: www.elsevier.com/locate/hbpd

Original Article/Liver

Insulin-like growth factor binding protein related protein 1 knockdown attenuates hepatic fibrosis via the regulation of MMPs/TIMPs in mice

Jun-Jie Ren[a], Ting-Juan Huang[a], Qian-Qian Zhang[a,b,c], Hai-Yan Zhang[a,b,c], Xiao-Hong Guo[a,b,c], Hui-Qin Fan[a,b,c], Ren-Ke Li[d,e], Li-Xin Liu[a,b,c,*]

[a] Department of Gastroenterology and Hepatology, The First Clinical Hospital of Shanxi Medical University, Taiyuan 030001, China
[b] Experimental Center of Science and Research, The First Clinical Hospital of Shanxi Medical University, Taiyuan 030001, China
[c] Key Laboratory of Cell Physiology, Department of the Ministry of Education, Shanxi Medical University, Taiyuan 030001, China
[d] Division of Cardiovascular Surgery, Toronto General Research Institute, University Health Network, Ontario, Canada
[e] Division of Cardiac Surgery, Department of Surgery, University of Toronto, Ontario, Canada

ARTICLE INFO

Article history:
Received 21 April 2018
Accepted 30 July 2018
Available online 29 August 2018

Keywords:
Hepatic fibrosis
Insulin-like growth factor binding protein related protein 1
Matrix metalloproteinase
Tissue inhibitor of metalloproteinase
Ultrasound-targeted microbubble destruction
Hedgehog signaling pathway

ABSTRACT

Background: Previous research suggested that insulin-like growth factor binding protein related protein 1 (IGFBPrP1), as a novel mediator, contributes to hepatic fibrogenesis. Matrix metalloproteinases (MMP) and tissue inhibitors of metalloproteinases (TIMP) play an essential role in hepatic fibrogenesis by regulating homeostasis and remodeling of the extracellular matrix (ECM). However, the interaction between IGFBPrP1 and MMP/TIMP is not clear. The present study was to knockdown IGFBPrP1 to investigate the correlation between IGFBPrP1 and MMP/TIMP in hepatic fibrosis.

Methods: Hepatic fibrosis was induced by thioacetamide (TAA) in mice. Knockdown of IGFBPrP1 expression by ultrasound-targeted microbubble destruction-mediated CMB-shRNA-IGFBPrP1 delivery, or inhibition of the Hedgehog (Hh) pathway by cyclopamine treatment, was performed in TAA-induced liver fibrosis mice. Hepatic fibrosis was determined by hematoxylin and eosin and Sirius red staining. Hepatic expression of IGFBPrP1, α-smooth muscle actin (α-SMA), transforming growth factor β 1 (TGFβ1), collagen I, MMPs/TIMPs, Sonic Hedgehog (Shh), and glioblastoma family transcription factors (Gli1) were investigated by immunohistochemical staining and Western blotting analysis.

Results: We found that hepatic expression of IGFBPrP1, TGFβ1, α-SMA, and collagen I were increased longitudinally in mice with TAA-induced hepatic fibrosis, concomitant with MMP2/TIMP2 and MMP9/TIMP1 imbalance and Hh pathway activation. Knockdown of IGFBPrP1 expression, or inhibition of the Hh pathway, reduced the hepatic expression of IGFBPrP1, TGFβ1, α-SMA, and collagen I and re-established MMP2/TIMP2 and MMP9/TIMP1 balance.

Conclusions: Our findings suggest that IGFBPrP1 knockdown attenuates liver fibrosis by re-establishing MMP2/TIMP2 and MMP9/TIMP1 balance, concomitant with the inhibition of hepatic stellate cell activation, down-regulation of TGFβ1 expression, and degradation of the ECM. Furthermore, the Hh pathway mediates IGFBPrP1 knockdown-induced attenuation of hepatic fibrosis through the regulation of MMPs/TIMPs balance.

Introduction

Hepatic fibrosis (HF) is overly exuberant wound healing in which excessive connective tissue builds up in the liver following acute or chronic liver injury. The activation of hepatic stellate cells (HSC) and their excessive secretion and deposition of extracellular matrix (ECM) [1], particularly collagen deposition, result in liver fibrosis and ultimately in cirrhosis or hepatocellular carcinoma. Therefore, understanding the pathogenesis of liver fibrosis is important for the preventive and antifibrotic therapies.

Insulin-like growth factor binding protein related protein 1 (IGFBPrP1), also known as IGFBP7, has been implicated in a

* Corresponding author at: Department of Gastroenterology and Hepatology and Experimental Center of Science and Research, The First Clinical Hospital of Shanxi Medical University; Key Laboratory of Cell Physiology, Department of the Ministry of Education, Shanxi Medical University, Taiyuan 030001, China.
E-mail address: lixinliu6@hotmail.com (L.-X. Liu).

https://doi.org/10.1016/j.hbpd.2018.08.008
1499-3872/

number of biological processes, including cell proliferation, differentiation, adhesion, senescence, and apoptosis [2–6]. It has previously been shown that IGFBPrP1 is a novel mediator involved in hepatic fibrogenesis. IGFBPrP1 can activate HSCs, which produce α-smooth muscle actin (α-SMA), and play an important role in the secretion and deposition of ECM [7–10]. In addition, IGFBPrP1 can further induce the expression of transforming growth factor β 1 (TGFβ1), the most prominent effector of liver fibrosis. IGFBPrP1 and TGFβ1 may be mutually regulated, resulting in activation of HSC and ECM deposition [11]. IGFBPrP1 is a potential therapeutic target for hepatic fibrosis.

The ECM is sustained by precisely regulated turnover, which is controlled by matrix metalloproteinases (MMP) and tissue inhibitors of metalloproteinases (TIMP) [12]. MMPs are the major enzymes implicated in ECM degradation [13], and TIMPs are secreted molecules that bind reversibly to MMPs in a 1:1 stoichiometric ratio. The balance between MMPs and TIMPs regulates ECM turnover and remodeling during both normal development and pathogenesis [14,15]. Accumulating evidence indicates that MMP/TIMP balance may play an essential role in hepatic fibrogenesis [12]. In the fibrotic liver, MMP/TIMP imbalance, along with HSC activation, occurred followed by progressive accumulation of ECM [1,16,17]. It is not clear whether IGFBPrP1 induced ECM deposition is via MMP/TIMP system.

An increasing number of studies indicate that the Hedgehog (Hh) pathway plays an important role in the pathogenesis and progression of liver fibrosis [18,19]. Hh ligand family members (Sonic Hh [Shh], Indian Hh, and Desert Hh) activate Hh signaling by engaging the transmembrane receptor, Patched (Ptc), on the surface of Hh-responsive cells. These include resident hepatic immune cells, stellate cells, and progenitors. Binding of Hh ligands to Ptc prevents Ptc from inhibiting Smoothened (Smo). Activated Smo controls cellular accumulation and nuclear localization of glioblastoma (Gli) family transcription factors (Gli1, Gli2, and Gli3) that regulate the expression of Hh-regulated genes modulating the proliferation, differentiation, and survival of Hh-responsive cells [18]. Our previous studies have found that IGFBPrP1 leads to HSC activation, ECM synthesis, and promotes the development of liver fibrosis via Hh pathway activation [7]. However, the mechanisms by which IGFBPrP1, MMP/TIMP balance, and the Hh signaling pathway regulate and interact with each other are not clear.

The use of ultrasound-targeted microbubble destruction (UTMD) as a stimulus for gene transfer offers significant advantages over other gene transfer modalities for application in gene-based therapies. Microbubbles, which were designed for molecular imaging and are used as ultrasound contrast agents for visualizing perfusion, have recently been used as a vehicle for delivering genes, proteins, or drugs because of their visibility in the target tissue [20,21]. Cationic microbubbles (CMB) with a positively charged surface can carry an adequate amount of plasmid to achieve a therapeutic effect. They have been shown to enhance gene delivery by UTMD [22–25]. In our study, we used UTMD with CMB to enhance gene transfection efficacy in mice livers.

Thioacetamide (TAA) is a hepatotoxic chemical that effectively induces hepatic fibrosis in experimental rodent models [26,27]. The pathophysiological processes of a rodent model with hepatic fibrosis induced by TAA closely resembles those observed in human with alcoholic or viral infection-induced liver fibrosis [28,29]. Therefore, in this study, we created a TAA-induced hepatic fibrosis mouse model to test the hypothesis that UTMD-mediated CMB-short hairpin RNAs (shRNA)-IGFBPrP1 delivery attenuates TAA-induced hepatic fibrosis by regulating the MMP2/TIMP2 and MMP9/TIMP1 balance via the hedgehog pathway.

Methods

Animals and TAA administration

Male wild-type C57BL/6 mice, 5–6 weeks old and weighing 18–22 g, were obtained from the Institute of Laboratory Animals at the Military Academy of Medical Sciences (Beijing, China). They were maintained in a temperature-controlled environment (20–22 °C) with a 12 h light–dark cycle, free access to drinking water, and ad libitum standard chow at the Department of Pharmacology of Shanxi Medical University. Mice were subjected to experimental procedures approved by the Animal Care and Use Committee of Shanxi Medical University and in accordance with the Guidelines on the Care and Use of Animals provided by the American Physiological Society.

C57BL/6 wild-type mice ($n=168$) were randomly divided into the normal group ($n=24$): normal breeding; control group ($n=24$): intraperitoneal injection of phosphate buffered solution (PBS) 0.1 mL/10 g, three times a week; TAA group ($n=24$): intraperitoneal injection of 100 mg/kg body weight of TAA (Sigma, St. Louis, MO, USA) dissolved in PBS three times a week; TAA + shRNA-NC group ($n=24$): one week following the first administration of TAA, the CMB-shRNA-NC solution was infused into the tail vein, simultaneously, and an ultrasound beam was delivered to UTMD; TAA + shRNA-IGFBPrP1 group ($n=24$): one week following the first administration of TAA, the CMB-shRNA-IGFBPrP1 solution was infused into the tail vein, simultaneously, and an ultrasound beam was delivered to UTMD; TAA + vehicle group ($n=24$): one week following the first administration of TAA, intraperitoneal injection of vehicle (10% DMSO + 30% PEG 300 + 5% Tween 80 + ddH_2O) 0.15 mL/10 g/d for 2 weeks; TAA + cyclopamine group ($n=24$): one week following the first administration of TAA, mice were intraperitoneally injected daily with 15 mg/kg cyclopamine (Selleck Chemicals, Houston, USA), a specific Hedgehog inhibitor, dissolved in vehicle for two weeks.

At week 2, 4, and 6 after the first administration of TAA, the animals were sacrificed for further analysis. Liver tissue and blood samples were harvested at these time points. Tissues were flushed with normal saline, snap frozen in liquid nitrogen, and stored at −80 °C until used for further assessment.

Cell culture and shRNA-IGFBPrP1 expressing plasmid transfection

The NIH/3T3 cell line (Cell Resource Center of Shanghai Institute of Life Sciences, Chinese Academy of Sciences, Shanghai, China) was cultured in RPMI 1640 medium (Gibco, New York, USA) supplemented with 10% fetal bovine serum, 100 U/mL penicillin, and 100 g/mL streptomycin. Plasmids coding for three shRNAs targeting mouse IGFBPrP1 mRNA and a scrambled shRNA as the negative control (shRNA-NC) were designed using software and synthesized by the Sangon Biotech Company (Shanghai, China). They were used to transfect NIH/3T3 cell lines using Lipofectamine 2000 (Invitrogen, Carlsbad, CA, USA). After transfection of the shRNA plasmid into the NIH/3T3 cells for 72 h, the most effective shRNA-IGFBPrP1 was selected. Both shRNA-IGFBPrP1 and shRNA-NC contained a green fluorescent protein (GFP) marker, which was used to determine transfection efficacy.

Plasmid shRNA-IGFBPrP1 and microbubble solutions

CMBs (USphere^{TM} Trans+) (Trust Bio-sonics Company, Taiwan, China) were used for gene transfection. To activate CMBs, the vial

was warmed to room temperature (20–30 °C) and oscillated for 40 s in an UltraMix™ (Monitex Company, Taiwan, China). ShRNA-IGFBPrP1 or shRNA-NC plasmids (40 μg) were added to CMBs (100 μL), and mixed well using a vortex. Solutions were then incubated at 4 °C for at least 15 min. The plasmid microbubble solution (100 μL) was diluted with sterilized saline to a total volume of 2.5 mL. Dilution was performed just prior to injection to prevent degradation.

UTMD-mediated gene delivery

Six days following the first administration of TAA, mice were anesthetized by intraperitoneal injection of chloral hydrate (400 mg/kg body weight), and the plasmid microbubble solution was injected into the tail vein slowly. A Prospect High Resolution Imaging System and 40 MHz transducer (S-Sharp Company, Taipei, Taiwan, China) were used to visualize the liver. Immediately following injection, an ultrasound beam was delivered with an M3S transducer that was situated precisely over the liver to destroy bubbles across this region using the Vivid 7 system (GE Healthcare, Chicago, USA) operating in the second harmonic mode (transmit: 1.7 MHz; receive: 3.4 MHz). Microbubble destruction was carried out for 5 min with a pulse cycle of 10 s on and 5 s off. The transmission depth was set at 2 cm, and a mechanical index of 0.9 was employed. Each ultrasound burst eliminated a large number of the microbubbles in the liver, and a pulsing interval of 5 s was used to allow replenishment of the microbubbles before the next burst. This method has previously been employed for UTMD gene delivery to the liver using CMB [30].

Western blotting analysis

Total protein (50 μg) was separated by SDS-PAGE and transferred to PVDF membranes (Bio-Rad Laboratories, Hercules, CA, USA). The membranes were probed with primary antibodies for IGFBPrP1 (1:1000, ab74169, Abcam, Cambridge, United Kingdom), α-SMA (1:500, ab5694, Abcam), collagen I (1:300, ab34710, Abcam), TGFβ1 (1:500, ab92486, Abcam), MMP2 (1:1000, ab92536, Abcam), MMP9 (1:1000, ab38898, Abcam), TIMP1 (1:500, Abcam), TIMP2 (1:1000, Abcam), Shh (1:500, Abcam), Gli1 (1:500, Sangon Biotech, Shanghai, China), and β-actin (1:1000, Abcam), followed by the incubation with secondary antibodies (1:5000). Blots were visualized using an enhanced chemiluminescence system after incubation with appropriate horseradish peroxidase-conjugated secondary antibodies [7]. Proteins were detected by enhanced chemiluminescence (ECL; Bio-Rad Laboratories). Specific signals were scanned using scanning densitometry and relative protein levels were determined with Quantity One Image software (Bio-Rad). For quantification, blots from at least three independent experiments were used.

Histological analysis and immunohistochemical staining

All paraffin-embedded liver tissues were cut into 4 μm thick sections and stained with hematoxylin and eosin (H&E) or Sirius Red stain for histological examination or collagen deposition, respectively.

Immunohistochemical staining was performed to examine the expression of protein in liver tissues. Briefly, endogenous peroxidase activities were blocked with 0.3% H_2O_2. Tissue sections were revived in a microwave oven with 10 mM sodium citrate buffer (pH 6.0) for 25 min and incubated at 37 °C for 1 h with primary antibodies: MMP2 (1:500), MMP9 (1:500), TIMP1 (1:200), TIMP2 (1:50), Gli (1:60), Shh (1:400). Sections were washed and incubated with biotinylated secondary antibody (ZSGB-BIO, Beijing, China). For negative controls, the primary antibodies were substituted with PBS. Visualization was carried out with a streptavidin biotin immunoperoxidase staining system (LSAB kit, Dako, USA) using 3, 3-diaminobenzidine (Sigma, St. Louis, MO, USA) as a chromogenic substrate.

For observation of GFP fluorescence, frozen liver sections were incubated with DAPI (Boster, Wuhan, China) for 5 min at room temperature and detected using a fluorescence microscope (BX43, Olympus, Tokyo, Japan) with an excitation wavelength of 488 nm.

Stained sections were viewed with an Olympus BX43 microscope and the results were analyzed with Image-Pro Plus 7.0 software. The results of immunoperoxidase staining, expressed as the integrated optical density (IOD) of the positive brown particles, were determined semi-quantitatively by examining 5 fields randomly at 400 × magnification in each slice. The results from Sirius Red staining were expressed as the percentage of the area occupied by the signal.

Statistical analysis

All data were expressed as the median (range) unless otherwise indicated, and all calculations were made using SPSS 16.0 statistical software. Statistical significance was evaluated using Mann-Whitney U test. In addition, the Spearman correlation coefficients (r values) were calculated. Results were considered statistically significant at $P < 0.05$.

Results

Expression of IGFBPrP1, TGFβ1, and α-SMA in livers of mice with TAA-induced hepatic fibrosis

Compared with the normal and PBS-treated groups, H&E staining of the livers from TAA treated mice showed increases in centrilobular necrosis, steatosis, hydropic degeneration, and bile duct proliferation, as well as infiltration of immune cells and inflammatory cells into the hepatic parenchyma (Fig. 1A). Sirius Red staining showed that collagen fibrils were mostly distributed in the portal and central vein areas week 2 after the first administration of TAA, and then gradually expanded and extended over time (Fig. 1B).

Following treatment with TAA, IGFBPrP1 levels in liver were gradually increased compared to levels in the normal and PBS-treated groups (Fig. 1G). The dynamic hepatic expression of α-SMA, TGFβ1, and collagen I in the liver was determined using Western blotting analysis. The results revealed that the HSC markers α-SMA and TGFβ1, which are the strongest cytokines involved in liver fibrosis, and collagen I, which is the main component of the ECM, were longitudinally increased in the TAA-treated mice compared to the normal and PBS-treated group at week 2, 4, and 6 (Fig. 1G, H).

MMPs/TIMPs imbalance in the livers of mice with TAA-induced hepatic fibrosis

MMPs and TIMPs contribute to both the progression and regression of liver fibrosis [12]. After the mice were treated with TAA, the expressions of MMP2 and MMP9 were significantly and gradually increased. The levels of MMP9 inhibitor TIMP1 and MMP2 inhibitor TIMP2 were also higher at week 2, 4, and 6 than in the normal and PBS-treated mice (Fig. 1C and G). The IGFBPrP1 levels showed a positive correlation with MMP2, TIMP2, MMP9, and TIMP1 expression in the fibrotic liver (r = 0.891, 0.931, 0.954, 0.965, respectively) (Fig. 1E and F). A change in either MMP or TIMP levels could alter the MMP/TIMP ratio and cause ECM degradation or accumulation. Consequently, the ratio of MMP2/TIMP2 was increased at week 4, while decreased at week 6, but still higher than the normal group;

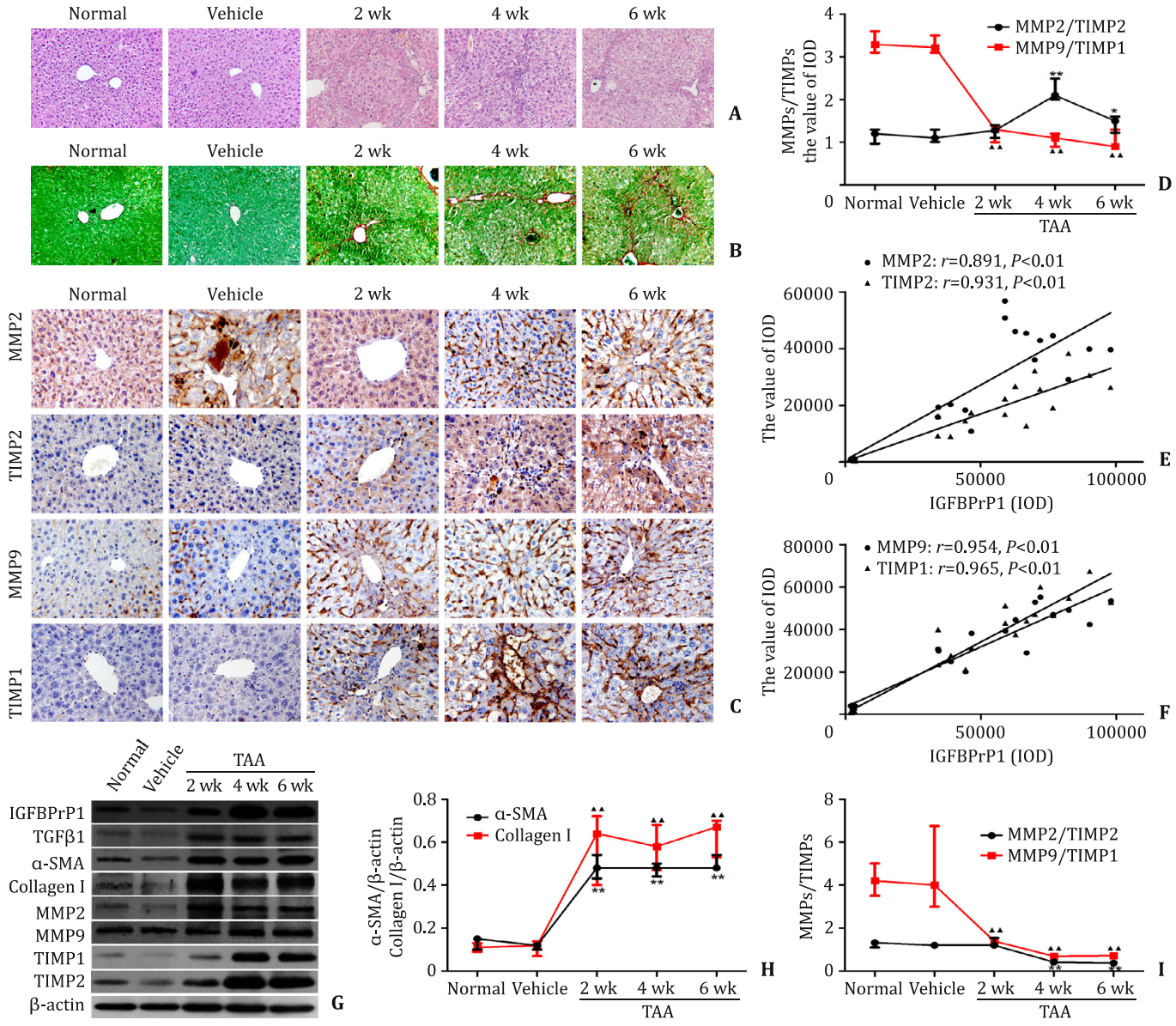

Fig. 1. Expression of IGFBPrP1, TGFβ1, α-SMA, collagen I, and the MMP/TIMP balance in the livers of mice with TAA-induced hepatic fibrosis. **A:** Histological analysis by H&E (original magnification × 200); **B**: Sirius Red staining (original magnification × 200); **C:** Immunohistochemical staining of MMP2, TIMP2, MMP9, and TIMP1 (original magnification × 400); **D:** The dynamic changes in the MMP/TIMP ratio; **E** and **F:** Correlation between the expression of IGFBPrP1 and MMP/TIMP at different time points; **G** and **H:** Western blotting of IGFBPrP1,TGFβ1, α-SMA, collagen I, and MMPs/TIMPs protein among different groups; **I:** Western blotting for MMP/TIMP ratio. β-actin and PBS acted as internal and negative controls, respectively. Data are presented as the median (range) ($n = 8$ per group) *: $P < 0.05$, **: $P < 0.01$, ▲: $P < 0.05$, ▲▲: $P < 0.01$, compared with the normal group.

and the MMP9/TIMP1 ratio was decreased at week 2, 4, and 6 using immunohistochemical staining (Fig. 1D). For Western blotting analysis (Fig. 1I), the ratio of MMP2/TIMP2 was not changed at week 2, but decreased at week 4 and 6, and the MMP9/TIMP1 ratio was decreased during all time points.

Knockdown of IGFBPrP1 expression reduces the expressions of α-SMA, TGFβ1, and collagen I in the livers of mice with TAA-induced hepatic fibrosis

Assessment of the accumulation of microbubbles in the liver after intravenous injection of CMB indicated that the microbubbles were accumulated in 10 s and then decreased and disappeared in 5 min (Fig. 2A). The mice were treated with UTMD-mediated shRNA-IGFBPrP1 delivered by CMB, while liver sections showed bright green fluorescence by fluorescence microscopy that peaked at week 4 and was mostly dissipated at week 6 after TAA administration. After the mice were treated with the shRNA-IGFBPrP1, their IGFBPrP1 protein levels gradually decreased over the period from week 2 to week 6 compared with levels in the shRNA-NC groups (Fig. 2D). Meanwhile, decreased α-SMA, TGFβ1, and collagen I expression was detected, indicating HSC activation was inhibited, ECM degraded, and liver fibrosis ameliorated compared with the shRNA-NC groups (Fig. 2D and E).

Knockdown of IGFBPrP1 expression reverts MMP2/TIMP2 and MMP9/TIMP1 imbalance in the livers of mice with TAA-induced hepatic fibrosis

After shRNA-IGFBPrP1 infection, the expression levels of the MMP2 and MMP9 proteins were increased and TIMP1 and TIMP2 decreased, compared with levels in the shRNA-NC groups at week

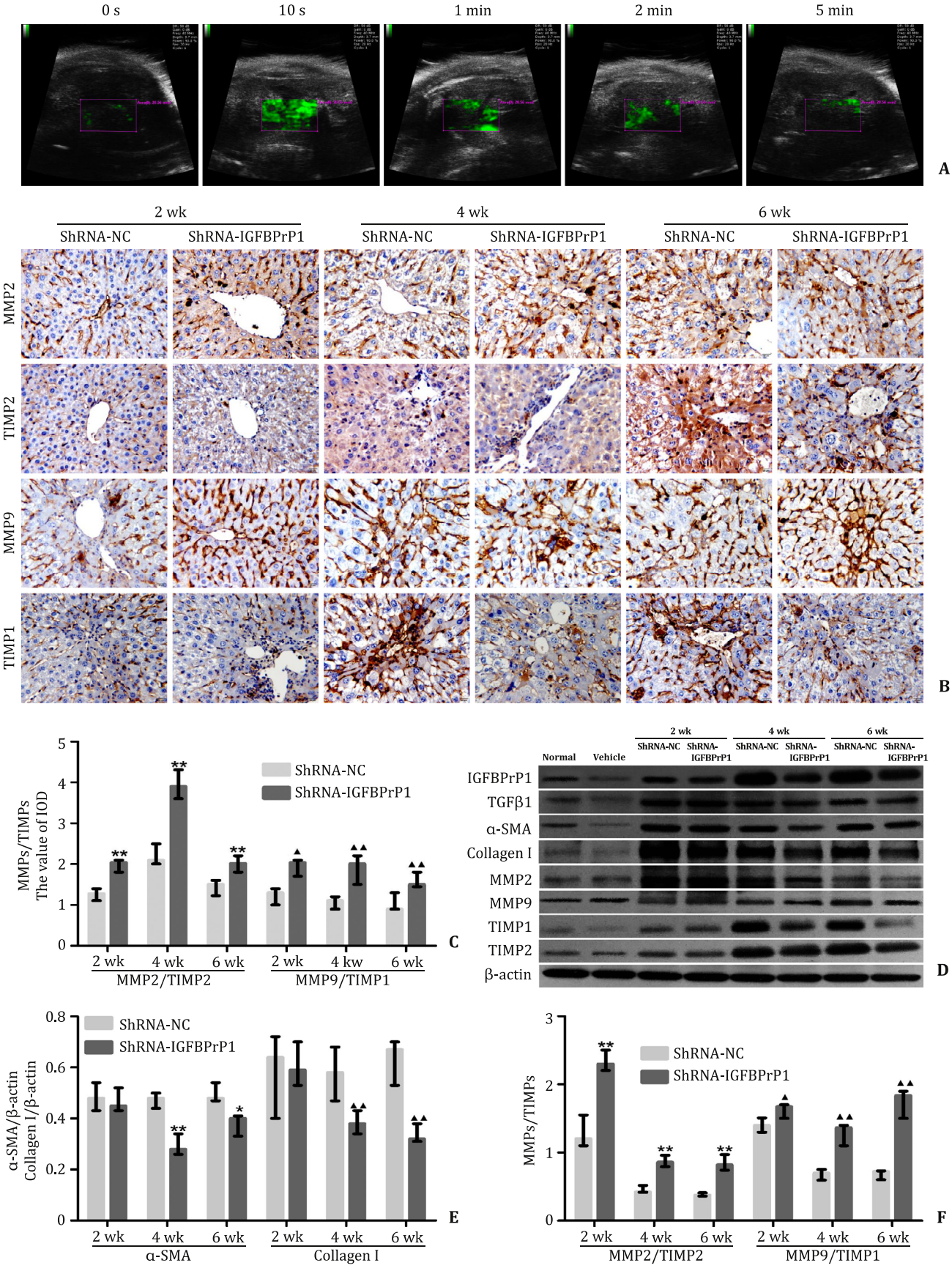

Fig. 2. Knockdown of IGFBPrP1 expression resulted in changes in the expression levels of α-SMA, TGFβ1, collagen I, and the MMP/TIMP balance in the livers of mice with TAA-induced hepatic fibrosis. **A:** The accumulation of CMB in the liver; **B:** Immunohistochemical staining of MMP2, TIMP2, MMP9, and TIMP1 (original magnification $\times$ 400); **C:** Immunohistochemical staining for the changes in the MMP/TIMP ratio; **D, E:** The comparison of IGFBPrP1, TGFβ1, α-SMA, collagen I, and MMPs/TIMPs protein among different groups; **F:** Western blotting for MMP/TIMP ratio. Data were presented as the median (range) ($n = 8$ per group) *: $P < 0.05$, **: $P < 0.01$, ▲: $P < 0.05$, ▲▲: $P < 0.01$, compared with the ShRNA-NC group.

2, 4, and 6 (Fig. 2B and D). Consequently, the MMP2/TIMP2 and MMP9/TIMP1 ratios were increased (Fig. 2C and F), benefiting the regression of ECM and the reversal of hepatic fibrosis.

IGFBPrP1 regulates the MMP2/TIMP2 and MMP9/TIMP1 balances via the Hh pathway in the livers of mice with TAA-induced hepatic fibrosis

To assess the expression levels of Hh-related protein in TAA-induced liver fibrosis, we evaluated the expression of the Shh and Gli1 proteins in mice livers. We found that hepatic expressions of the Shh and Gli1 proteins were gradually increased in mice treated with TAA compared to mice from the normal and PBS-treated groups at week 2, 4, and 6 (Fig. 3A and B). The IGFBPrP1 levels showed a positive correlation with Shh and Gli1 expression in livers with hepatic fibrosis induced by TAA ($r = 0.910$ and 0.926, respectively) (Fig. 3C).

Following treatment with UTMD-mediated shRNA-IGFBPrP1 delivery via CMB, hepatic expression of Shh and Gli1 in mice was inhibited significantly compared to shRNA-NC groups at week 2, 4, and 6, and hepatic expression of Gli1 was inhibited at week 4 and 6 (Fig. 3D–F).

Cyclopamine inhibits the Hedgehog signaling pathway [31]. After mice with liver fibrosis were treated with cyclopamine, there was a reduction in the protein levels of Shh and Gli1 ($P < 0.05$) (Fig. 4A, B, D), and a concomitant decrease in the expression of α-SMA, TGFβ1, and collagen I protein in comparison to the vehicle-treated group ($P < 0.05$) (Fig. 4D and E). However, expression of the IGFBPrP1 protein did not significantly differ between the cyclopamine-treated and vehicle-treated groups ($P > 0.05$) (Fig. 4D). After cyclopamine administration, MMP2 and MMP9 protein expressions were increased while TIMP1 and TIMP2 expressions were decreased compared with vehicle groups at week 2, 4, and 6 ($P < 0.05$) (Fig. 4A and D). Consequently, the MMP2/TIMP2 and MMP9/TIMP1 ratios were increased (Fig. 4C and F).

Discussion

Previous research suggested that IGFBPrP1 contributes to hepatic fibrogenesis [7–10]. However, the detailed profibrogenic mechanism by which IGFBPrP1 acts is not yet completely understood. In the present study, we further explored the mechanism by which MMP/TIMP balance is regulated by IGFBPrP1 in a hepatic fibrosis model. Our results showed that IGFBPrP1 promoted hepatic fibrogenesis by regulating the MMP2/TIMP2 and MMP9/TIMP1 balances via the Hh pathway in the livers of mice with TAA-induced hepatic fibrosis.

A hepatic-fibrosis model was successfully established in mice through TAA administration three times a week for 6 weeks which was consistent with the literature [26]. While investigating IGFBPrP1 expression in the livers of fibrotic mice by means of immunohistochemical staining and Western blotting, we found that IGFBPrP1 levels gradually increased with time. Additionally, hepatic expression of α-SMA, TGFβ1, and collagen I in TAA-treated mice showed a marked increase during fibrogenesis. These results were in agreement with our previous findings, which showed that IGFBPrP1 plays an important role in several mechanisms of liver fibrogenesis, including activation of HSC, up-regulation of TGFβ1, and secretion and deposition of ECM [9,10].

The imbalance between MMPs and TIMPs causes pathologic ECM deposition in liver fibrosis [12]. In this study, TAA treatment induced substantially increased MMP2 and MMP9 expression in the liver. The expression and function of MMPs are regulated by different TIMPs. We found that MMP2, MMP9, TIMP1, and TIMP2 were all increased in fibrotic livers. Our data also revealed that the ratio of MMP2/TIMP2 was increased at week 4, while decreased at week 6, but still higher than the normal group, and that the MMP9/TIMP1 ratio was decreased at week 2, 4, and 6. The results obtained by the two different experimental methods are not completely consistent which might be related with different specimen collection area or small sample size. During the early stage, the immovable or increased ratio of MMP2/TIMP2 may destroy the basement membrane and ECM, providing the proper microenvironment for HSC activation. A decreased MMP/TIMP ratio may contribute to the secretion and deposition of ECM and promote liver fibrosis. Our results are in agreement with reports that the MMP/TIMP balance was broken in hepatic fibrosis induced by hepatotoxicity drugs [32,33]. In addition, IGFBPrP1 levels were also positively correlated with MMPs and TIMPs levels. These results suggest that an imbalance of MMP2/TIMP2 and MMP9/TIMP1 play a role in IGFBPrP1-mediated hepatic fibrosis.

UTMD-mediated gene delivery using CMB improves the efficacy of gene delivery in a manner that may be clinically translated. It has been confirmed as a non-invasive, safe, low-cost, well-targeted, and repeatable method for gene transfection [25,34,35]. To further evaluate the relationship between IGFBPrP1 and the MMP/TIMP balance in hepatic fibrosis, we successfully used UTMD-mediated shRNA-IGFBPrP1 delivery with CMB to knockdown the IGFBPrP1 gene in livers with TAA-induced hepatic fibrosis. Furthermore, knockdown of IGFBPrP1 expression attenuated TAA-induced hepatic fibrosis and reduced the expression of α-SMA, TGFβ1, and collagen I. Added to this, overexpression of MMP2 and MMP9 and down-regulation of TIMP1 and TIMP2 were observed in IGFBPrP1 gene knockdown fibrotic livers. Consequently, the ratios of MMP2/TIMP2 and MMP9/TIMP1 were increased in livers in which IGFBPrP1 expression was significantly reduced. This suggests that the knockdown of IGFBPrP1 attenuates liver fibrosis via re-establishment the MMP2/TIMP2 and MMP9/TIMP1 balances, in conjunction with inhibition of HSC activation, down-regulated TGFβ1, and degradation of the ECM.

The Hh pathway is generally silent in healthy adult livers but is activated by factors associated with liver injury, which causes Hh ligands, and other related proteins, to be expressed significantly [36,37]. When Hh pathway activation is excessive and/or prolonged in injured livers, the result is chronic inflammation and fibrosis [19,38]. Comparable results were observed in our experiment. The productions of Shh and Gli1 proteins were increased in the fibrotic livers. In addition, hepatic expression of IGFBPrP1 protein was positively correlated with Shh and Gli1 expression. Furthermore, the hepatic expressions of Shh and Gli1 were decreased significantly in response to the knockdown of IGFBPrP1, thus confirming that the Hh pathway was inhibited. These results suggested that IGFBPrP1 expression leads to hepatic fibrosis via Hh pathway activation.

Cyclopamine is a natural plant extracted from corn lilies that downregulates Hh signals through direct inhibition of the SMO receptor [39,40]. After cyclopamine treatment of mice with lowered hepatic expression of Shh and Gli1, inhibition of the Hh pathway reduced the hepatic expression of α-SMA, TGFβ1, and collagen I, but did not affect the expression of IGFBPrP1. Furthermore, cyclopamine-mediated inhibition of the Hh pathway enhanced the expressions of MMP2 and MMP9 and inhibited TIMP1 and TIMP2 expression, altering the MMP2/TIMP2 and MMP9/TIMP1 ratios. Collectively, IGFBPrP1 did not directly regulate expression of either MMP or TIMP. IGFBPrP1, as an upstream regulator of Hh signaling, promoted Hh signaling which could disturb MMP/TIMP balance. These results confirmed that inhibition of the Hh pathway attenuated HSC activation and TGFβ1 expression, remodeled ECM, and re-established the MMP/TIMP balance in mice with IGFBPrP1-mediated liver fibrosis.

The present study has several limitations. Although the results suggested that the mechanisms may involve inhibition of Hh

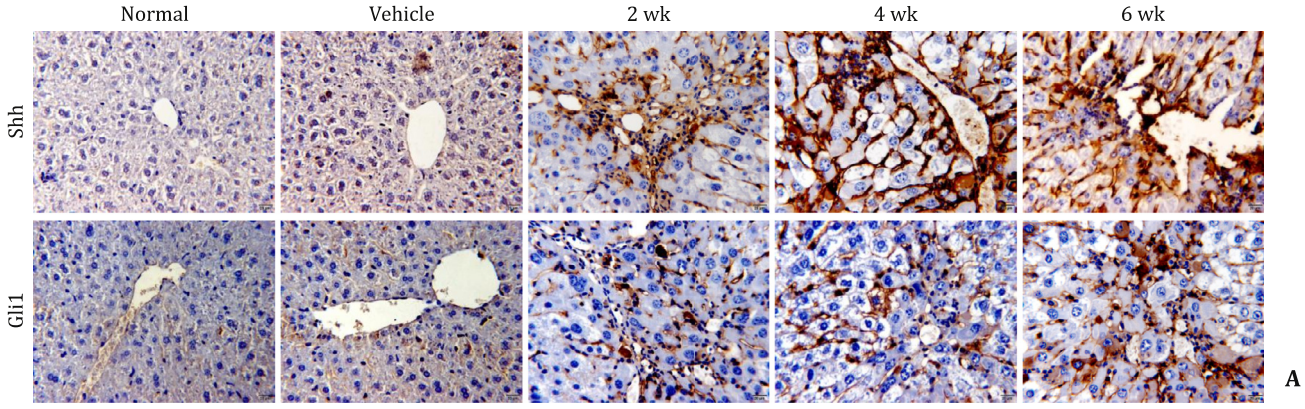

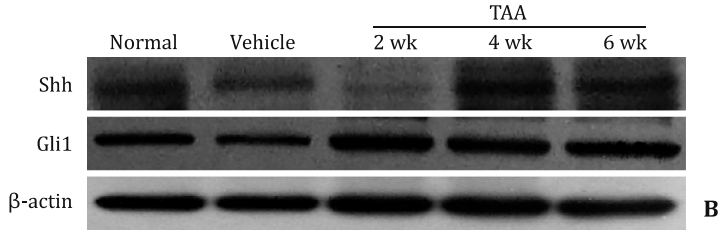

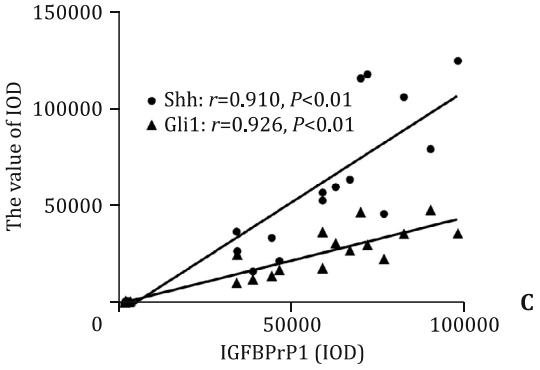

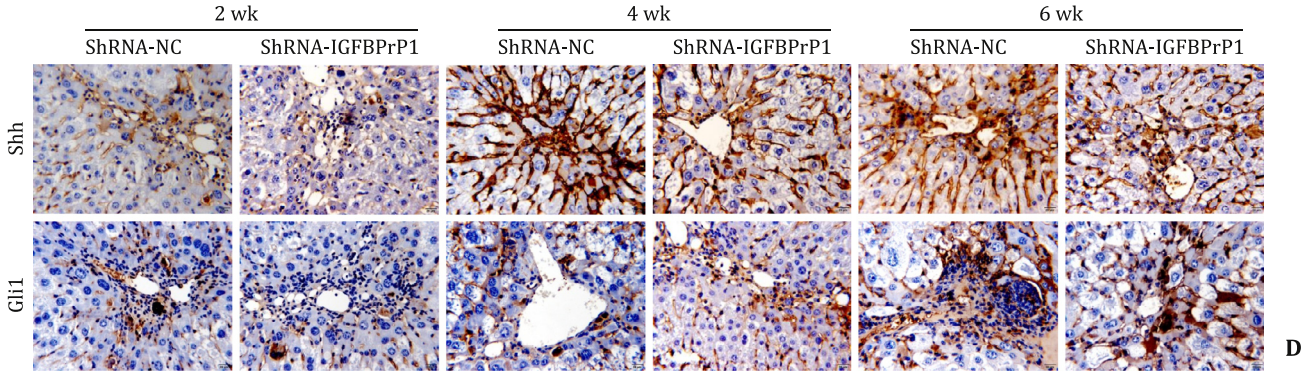

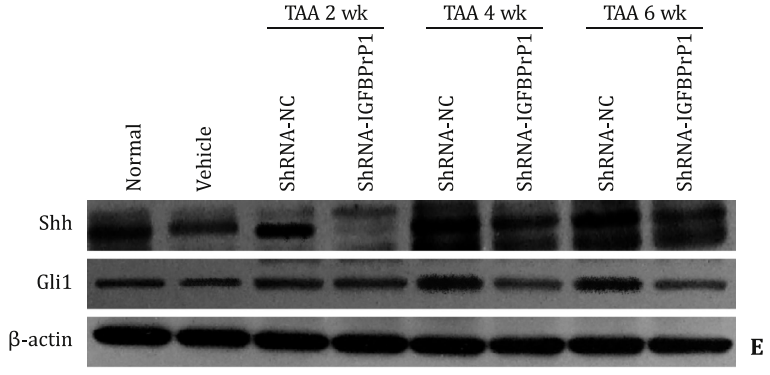

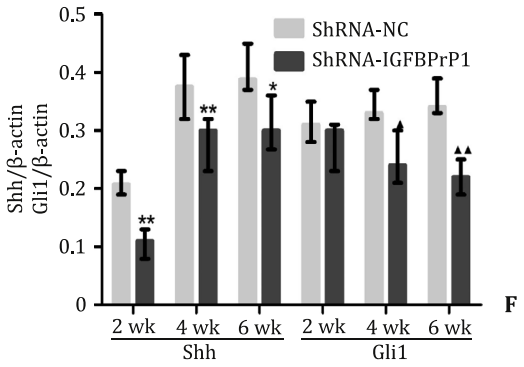

Fig. 3. Knockdown of the expression of IGFBPrP1 resulted in changes in Shh and Gli1 expression in the livers of mice with TAA-induced hepatic fibrosis. **A:** Immunohistochemical staining of Shh and Gli1 (original magnification × 400); **B:** Western blotting for Shh and Gli1 protein; **C:** Relationship between the expression of IGFBPrP1, Shh, and Gli1 at multiple time points; **D:** The comparison of Shh and Gli1 among different groups; **E** and **F:** Western blotting for the changes of Shh and Gli1 with IGFBPrP1 knockdown. Data are presented as median (range) ($n = 8$ per group) *: $P < 0.05$, **: $P < 0.01$, ▲: $P < 0.05$, ▲▲: $P < 0.01$, compared with the normal or ShRNA-NC groups.

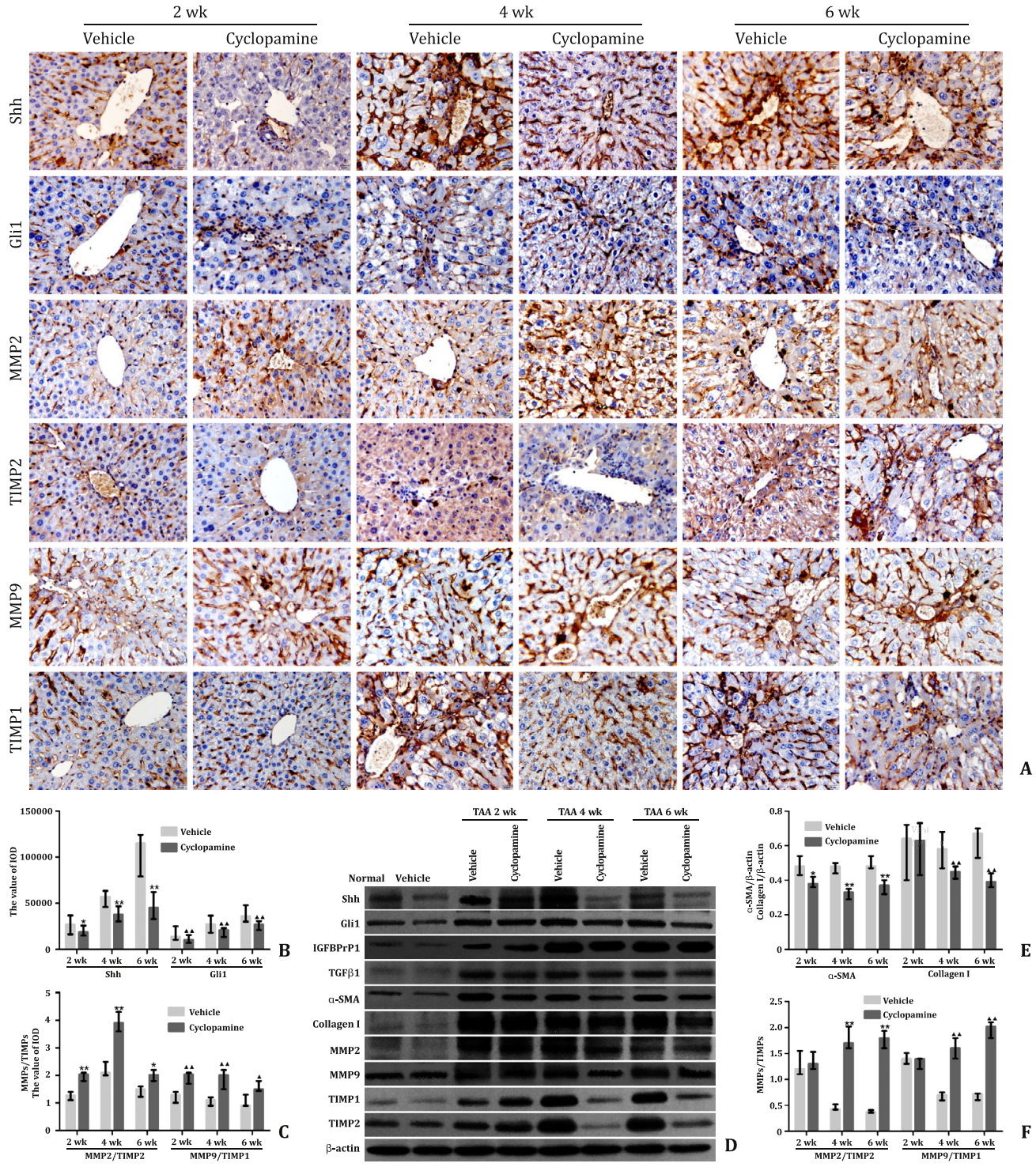

Fig. 4. Expression of Shh, Gli1, IGFBPrP1, TGFβ1, α-SMA, collagen I, and MMP/TIMP in the livers of mice with TAA-induced hepatic fibrosis after cyclopamine treatment. **A** and **B:** The comparison of Shh, Gli1, and MMPs/TIMPs protein among different groups; **C:** Immunohistochemical staining for changes in MMP/TIMP ratio; **D** and **E:** The dynamic changes in Shh, Gli1, IGFBPrP1, TGFβ1, α-SMA, collagen I, and MMP/TIMP protein among different groups; **F:** Western blotting for the changes in the MMP/TIMP ratio. Data are presented as median (range) ($n = 8$ per group). *: $P < 0.05$, **: $P < 0.01$, ▲: $P < 0.05$, ▲▲: $P < 0.01$, compared with the vehicle group.

pathway control of MMP and TIMP expression, more experiments should be carried out to reveal the mechanism that how Hh signaling differentially regulates the expressions of MMPs and TIMPs, and how IGFBPrP1 regulates the expression of Shh and Gli1.

In conclusion, this study demonstrated that UTMD-mediated CMB-shRNA-IGFBPrP1 delivery attenuates TAA-induced hepatic fibrosis in mice by re-establishing the balance of MMP2/TIMP2 and MMP9/TIMP1, accompanied with inhibition of HSC activation, down-regulation TGFβ1, and degradation of the ECM. Furthermore, the Hh pathway participates in the mechanism by which IGFBPrP1 knockdown attenuates hepatic fibrosis through regulation of the MMP/TIMP balance. Our results suggest that IGFBPrP1 plays a crucial role in the hepatic fibrogenesis. We therefore encourage the evaluation of IGFBPrP1 as a potential therapeutic target for treating

liver fibrotic patients. UTMD therapy with CMB-shRNA-IGFBPrP1 is a feasible technology for targeted gene delivery in the treatment of hepatic fibrosis.

Acknowledgments

We thank Jin Wang, Kun Xu and Xiu-Qing Li for assisting with UTMD.

Contributors

LLX designed and proposed the study. RJJ analyzed the data and wrote the draft. RJJ, HTJ, ZQQ, ZHY, GXH and FHQ performed the experiments. LRK provided the theoretical and practical guidance of ultrasound-targeted microbubble destruction (UTMD). All authors contributed to the interpretation of the study and to further drafts. LLX is the guarantor.

Funding

This study was supported by grants from National Natural Science Foundation of China (81670559), Key Research and Development Project of Shanxi Province (201603D421023), Youth Fund of Shanxi Medical University (02201514), Graduate Student Education Innovation Project of Shanxi (2016BY077), and Youth Fund of Applied Basic Research Program of Shanxi (201701D221175).

Ethical approval

All institutional and national guidelines for the care and use of laboratory animals were followed in accordance with the Guidelines on the Care and Use of Animals provided by the American Physiological Society. The study was strictly conformed to the ethical rules of standard experimental animal studies, and was approved by the Ethics Committee of Shanxi Medical University (SCXK2009-0001).

Competing interest

No benefits in any form have been received or will be received from a commercial party related directly or indirectly to the subject of this article.

References

[1] Friedman SL. Evolving challenges in hepatic fibrosis. Nat Rev Gastroenterol Hepatol 2010;7:425–436.
[2] Chen D, Siddiq A, Emdad L, Rajasekaran D, Gredler R, Shen XN, et al. Insulin–like growth factor-binding protein-7 (IGFBP7): a promising gene therapeutic for hepatocellular carcinoma (HCC). Mol Ther 2013;21:758–766.
[3] Nousbeck J, Sarig O, Avidan N, Indelman M, Bergman R, Ramon M, et al. Insulin-like growth factor-binding protein 7 regulates keratinocyte proliferation, differentiation and apoptosis. J Invest Dermatol 2010;130:378–387.
[4] Wilson HM, Birnbaum RS, Poot M, Quinn LS, Swisshelm K. Insulin-like growth factor binding protein-related protein 1 inhibits proliferation of MCF-7 breast cancer cells via a senescence-like mechanism. Cell Growth Differ 2002;13:205–213.
[5] Benatar T, Yang W, Amemiya Y, Evdokimova V, Kahn H, Holloway C, et al. IGFBP7 reduces breast tumor growth by induction of senescence and apoptosis pathways. Breast Cancer Res Treat 2012;133:563–573.
[6] Tamura K, Hashimoto K, Suzuki K, Yoshie M, Kutsukake M, Sakurai T. Insulin-like growth factor binding protein-7 (IGFBP7) blocks vascular endothelial cell growth factor (VEGF)-induced angiogenesis in human vascular endothelial cells. Eur J Pharmacol 2009;610:61–67.
[7] Guo X, Zhang H, Zhang Q, Li X, Liu L. Screening for and validation of a hepatic fibrosis-related pathway induced by insulin-like growth factor-binding protein-related protein 1. Eur J Gastroenterol Hepatol 2016;28:762–772.
[8] Zhang Y, Zhang QQ, Guo XH, Zhang HY, Liu LX. IGFBPrP1 induces liver fibrosis by inducing hepatic stellate cell activation and hepatocyte apoptosis via Smad2/3 signaling. World J Gastroenterol 2014;20:6523–6533.
[9] Guo Y, Zhang Y, Zhang Q, Guo X, Zhang H, Zheng G, et al. Insulin-like growth factor binding protein-related protein 1 (IGFBPrP1) contributes to liver inflammation and fibrosis via activation of the ERK1/2 pathway. Hepatol Int 2015;9:130–141.
[10] Guo XH, Liu LX, Zhang HY, Zhang QQ, Li Y, Tian XX, et al. Insulin-like growth factor binding protein-related protein 1 contributes to hepatic fibrogenesis. J Dig Dis 2014;15:202–210.
[11] Li XQ, Zhang QQ, Zhang HY, Guo XH, Fan HQ, Liu LX. Interaction between insulin-like growth factor binding protein-related protein 1 and transforming growth factor beta 1 in primary hepatic stellate cells. Hepatobiliary Pancreat Dis Int 2017;16:395–404.
[12] Hemmann S, Graf J, Roderfeld M, Roeb E. Expression of MMPs and TIMPs in liver fibrosis - a systematic review with special emphasis on anti-fibrotic strategies. J Hepatol 2007;46:955–975.
[13] Parks WC, Wilson CL, López-Boado YS. Matrix metalloproteinases as modulators of inflammation and innate immunity. Nat Rev Immunol 2004;4:617–629.
[14] Sternlicht MD, Werb Z. How matrix metalloproteinases regulate cell behavior. Annu Rev Cell Dev Biol 2001;17:463–516.
[15] Chirco R, Liu XW, Jung KK, Kim HR. Novel functions of TIMPs in cell signaling. Cancer Metastasis Rev 2006;25:99–113.
[16] Roderfeld M, Hemmann S, Roeb E. Mechanisms of fibrinolysis in chronic liver injury (with special emphasis on MMPs and TIMPs). Z Gastroenterol 2007;45:25–33.
[17] Duarte S, Baber J, Fujii T, Coito AJ. Matrix metalloproteinases in liver injury, repair and fibrosis. Matrix Biol 2015;44-46:147–156.
[18] Omenetti A, Choi S, Michelotti G, Diehl AM. Hedgehog signaling in the liver. J Hepatol 2011;54:366–373.
[19] Choi SS, Omenetti A, Syn WK, Diehl AM. The role of Hedgehog signaling in fibrogenic liver repair. Int J Biochem Cell Biol 2011;43:238–244.
[20] Ferrara KW, Borden MA, Zhang H. Lipid-shelled vehicles: engineering for ultrasound molecular imaging and drug delivery. Acc Chem Res 2009;42:881–892.
[21] Geis NA, Katus HA, Bekeredjian R. Microbubbles as a vehicle for gene and drug delivery: current clinical implications and future perspectives. Curr Pharm Des 2012;18:2166–2183.
[22] Panje CM, Wang DS, Pysz MA, Paulmurugan R, Ren Y, Tranquart F, et al. Ultrasound-mediated gene delivery with cationic versus neutral microbubbles: effect of DNA and microbubble dose on in vivo transfection efficiency. Theranostics 2012;2:1078–1091.
[23] Wang DS, Panje C, Pysz MA, Paulmurugan R, Rosenberg J, Gambhir SS, et al. Cationic versus neutral microbubbles for ultrasound-mediated gene delivery in cancer. Radiology 2012;264:721–732.
[24] Sun L, Huang CW, Wu J, Chen KJ, Li SH, Weisel RD, et al. The use of cationic microbubbles to improve ultrasound-targeted gene delivery to the ischemic myocardium. Biomaterials 2013;34:2107–2116.
[25] Yan P, Chen KJ, Wu J, Sun L, Sung HW, Weisel RD, et al. The use of MMP2 antibody-conjugated cationic microbubble to target the ischemic myocardium, enhance Timp3 gene transfection and improve cardiac function. Biomaterials 2014;35:1063–1073.
[26] Liu Q, Zhang Y, Yang S, Wu Y, Wang J, Yu W, et al. PU.1-deficient mice are resistant to thioacetamide-induced hepatic fibrosis: PU.1 finely regulates Sirt1 expression via transcriptional promotion of miR-34a and miR-29c in hepatic stellate cells. Biosci Rep 2017:37.
[27] Crespo Yanguas S, da Silva TC, Pereira IVA, Willebrords J, Maes M, Sayuri Nogueira M, et al. TAT-Gap19 and carbenoxolone alleviate liver fibrosis in mice. Int J Mol Sci 2018:19.
[28] Lv J, Nie ZK, Zhang JL, Liu FY, Wang ZZ, Ma ZL, et al. Corn peptides protect against thioacetamide-induced hepatic fibrosis in rats. J Med Food 2013;16:912–919.
[29] Salguero Palacios R, Roderfeld M, Hemmann S, Rath T, Atanasova S, Tschuschner A, et al. Activation of hepatic stellate cells is associated with cytokine expression in thioacetamide-induced hepatic fibrosis in mice. Lab Invest 2008;88:1192–1203.
[30] Zhang SH, Wen KM, Wu W, Li WY, Zhao JN. Efficacy of HGF carried by ultrasound microbubble-cationic nano-liposomes complex for treating hepatic fibrosis in a bile duct ligation rat model, and its relationship with the diffusion-weighted MRI parameters. Clin Res Hepatol Gastroenterol 2013;37:602–607.
[31] Lee ST, Welch KD, Panter KE, Gardner DR, Garrossian M, Chang CW. Cyclopamine: from cyclops lambs to cancer treatment. J Agric Food Chem 2014;62:7355–7362.
[32] Park SY, Shin HW, Lee KB, Lee MJ, Jang JJ. Differential expression of matrix metalloproteinases and tissue inhibitors of metalloproteinases in thioacetamide-induced chronic liver injury. J Korean Med Sci 2010;25:570–576.
[33] Yang J, Zheng J, Wu L, Shi M, Zhang H, Wang X, et al. NDRG2 ameliorates hepatic fibrosis by inhibiting the TGF-β1/Smad pathway and altering the MMP2/TIMP2 ratio in rats. PLoS One 2011;6:e27710.
[34] Xu Y, Xie Z, Zhou Y, Zhou X, Li P, Wang Z, et al. Experimental endostatin-GFP gene transfection into human retinal vascular endothelial cells using ultrasound-targeted cationic microbubble destruction. Mol Vis 2015;21:930–938.
[35] Zhou Y, Gu H, Xu Y, Li F, Kuang S, Wang Z, et al. Targeted antiangiogenesis gene therapy using targeted cationic microbubbles conjugated with CD105 antibody compared with untargeted cationic and neutral microbubbles. Theranostics 2015;5:399–417.
[36] Verdelho Machado M, Diehl AM. The hedgehog pathway in nonalcoholic fatty liver disease. Crit Rev Biochem Mol Biol 2018;53:264–278.
[37] Shen X, Peng Y, Li H. The injury-related activation of Hedgehog signaling pathway modulates the repair-associated inflammation in liver fibrosis. Front Immunol 2017;8:1450.

[38] Bohinc BN, Diehl AM. Mechanisms of disease progression in NASH: new paradigms. Clin Liver Dis 2012;16:549–565.
[39] Zhang F, Hao M, Jin H, Yao Z, Lian N, Wu L, et al. Canonical hedgehog signalling regulates hepatic stellate cell-mediated angiogenesis in liver fibrosis. Br J Pharmacol 2017;174:409–423.
[40] Samatiwat P, Takeda K, Satarug S, Ohba K, Kukongviriyapan V, Shibahara S. Induction of MITF expression in human cholangiocarcinoma cells and hepatocellular carcinoma cells by cyclopamine, an inhibitor of the Hedgehog signaling. Biochem Biophys Res Commun 2016;470:144–149.